Journal of Pharmaceutical Research International

33(30B): 80-96, 2021; Article no.JPRI.69139
ISSN: 2456-9119
(Past name: British Journal of Pharmaceutical Research, Past ISSN: 2231-2919, NLM ID: 101631759)

Potential of Topical Cosmeceuticals Cream Functionalized with Biogenic Metallic Nanostructured Material as Antibacterial Agents

Rajesh Dodiya[1*], Mrunal K Shirsat[1] and Jitendra K Patel[1]

[1]Department of Pharmaceutical Science, Madhav University, Sirohi, 307001, Rajasthan, India.

Authors' contributions

This work was carried out in collaboration among all authors. Author RD conceptualization, experimental design, writing and editing the draft. Author MKS reading and editing the final draft, author JKP reading and editing the final draft. All authors read and approved the final manuscript.

Article Information

DOI: 10.9734/JPRI/2021/v33i30B31643
Editor(s):
(1) Dr. Giuseppe Murdaca, University of Genoa, Italy.
Reviewers:
(1) Enkelejda Goci, Aldent University, Albania.
(2) Martyna Zagórska-Dziok, University of Information Technology and Management in Rzeszow, Poland.
(3) Sandra Pucciarelli, University of Camerino,Italy.
Complete Peer review History: http://www.sdiarticle4.com/review-history/69139

Original Research Article

Received 25 March 2021
Accepted 31 May 2021
Published 04 June 2021

ABSTRACT

Aims: In this study, the phytochemical analysis of *Eucalyptus globulus* leaf was analyzed and used in synthesis of silver nanoparticles. The silver nanoparticle incorporated antimicrobial cosmeceutical cream was developed and characterized for physicochemical parameters, antimicrobial properties, and biocompatibility was evaluated.
Methodology: *E. globulus* aqueous leaf extract was preliminary analyzed for the presence of phytochemical and confirmed using thin layer chromatography techniques. Further, a green synthesis of silver nanoparticle was accomplished using aqueous leaf extract of *E. globulus.* The formation of nanoparticles was confirmed and characterized by UV-vis spectrophotometer, transmission electron microscopy, dynamic light scattering, zeta potential, X-ray diffractometer, field emission scanning electron microscopy, and fourier transform infrared spectroscopy. The nanoparticles were incorporated in cream and the antimicrobial property was evaluated using agar well diffusion method.
Results: The phyto-chemical evaluation of *E. globulus* aqueous leaf extract showed the presence of phenolic, tannins, saponnins, carbohydrate, and glycoside. Moreover, *Eucalyptus globulus*

**Corresponding author: E-mail: rajdodia7@gmail.com;*

aqueous leaf extract exhibited antioxidant activity in a dose dependent manner. The surface plasmon resonance peak was 424 nm and functional group such as hydroxyl, carboxyl, alkyl halides, amines, carbonyl, amide groups, and phenolic compounds were present which was important for the bio-reduction, stabilization, and capping of the silver nitrate into nanoparticles. Energy dispersive x-ray (EDX) analysis showed silver as the main element present and the nanoparticles were oval in shape and 19-60 nm in size with effective diameter of 90 nm. The test cream exhibited surface roughness of ≈ 30 nm, contact angle of ≈ 100, and surface energy of ≈88 mN/m. The formulated creams were consistent, with satisfactory pH, viscosity and spreadability.
Conclusion: The results demonstrated an eco-friendly and cost-effective approach to synthesis biogenic silver nanoparticles using aqueous extract of *E. globulus*. *Eucalyptus globulus* aqueous leaf extract stabilized and capped silver nanoparticles incorporated topical cream exhibited potent antimicrobial efficacy against *Staphylococcus aureus*, *Staphylococcus epidermidis*, and *Pseudomonas aeruginosa*.

Keywords: Silver nanoparticles; antibacterial cream; green synthesis; Eucalyptus globulus.

.

1. INTRODUCTION

Cosmeceuticals usage has been increased drastically over the years with fastest growing segment of the beauty and personal care products. Nanostructured incorporated cosmetic and skin care products gaining popularity in cosmetic industry. Cosmetics with engineered materials including gel [1], solid lipid nanoparticles [2], sunscreen nano-pigments [3], and nanoemulsions [4] have been reported for commercialization in global market. Cosmetics product incorporated with nanoparticles provide light scattering, tactile, and matte effects to end user. Metallic nanomaterials have been used to improve the performance of a wide range of cosmetic products, including moisturizer [5], anti-aging cream [6], hydrogel [1], and perfume base dermal dressings [7]. Nanostructures zinc oxide, titanium dioxide, zircornium dioxide, and cerium oxide are widely used in sunscreen to protect skin from UV radiation [8]. Silver nanoparticles had demonstrated improved antibacterial spectrum against wide range of medical important pathogens [9-12] and effective against atopic dermatitis, compared to silver nitrate. In addition, silver nanoparticles are effective as preservatives in cosmetics, and in anti-acne preparation [13].

Green synthesized metallic biocompatible nanomaterials are widely applied in biomedical science, due to unique physicochemical properties, controlled size, and shape [12]. Biomedical applications of chemically synthesized silver nanoparticles have been challenging due to the use of toxic and non-biodegradable materials. However, the synthesis of silver nanoparticles via green chemistry is an eco-friendly process and an emerging trend in the field of nanobiotechnology [14]. Plant extracts and microorganism waste are considered as an environmentally safe and cost-effective candidate for synthesis of metallic nanoparticles due to presence of bioactive constituents compared to chemical synthesis. Valorization of *Pichia* spent media [15] and gene based synthesis of silver nanoparticles reported a clean, convenient, and inexpensive approach with excellent antimicrobial property [16].

Since from ancient time, plants were used as herbal medicine in many parts of the world. In some countries tradition, several part of plant including leaf, roots, flowers, woods have a specific benefit as medicine. *Eucalyptus* genus is not only a plant that has advantage as a pulp, plywood, and solid wood production but studies had already reported that *Eucalyptus globulus* leaf has phyto-constituents that play an important role as therapeutic activities as chemotherapeutic [17,18], antidiabetic [19], antiseptic, antimicrobial [20,21], gastrointestinal disorder treatment, wound healing [22-24], insect repellent [25], herbicidal [26,27], acaricidal [28], nematicidal [29], perfume [30], soap making, grass remover, and other. The major compound of Eucalyptus is 1,8-cineole (approximately 70%) [31], a monoterpen that include in terpene group. On the other hand, *Eucalyptus* has been also reported for the presence of saponin, phenolic, and flavonoid [32,33]. Acylphloroglucinol an amphiphilic compound that has tail which is acyl (hydrophobic side) and head is pholoroglucinol (hydrophilic side) is one of compounds also present in *Eucalyptus* genus [34]. Hydrophilic head moiety binds with an intermolecular hydrogen bond like a “hook” attaching itself to a hydrophilic portion of the membrane, after which the hydrophobic tail portion of the molecule is

then able to enter into the membrane lipid bilayer. Hydrophobic tail penetrates deeper into the lipid, tail region of the membrane forming an amphiphilic conformation with the cationic group located at the hydrophobic water interface induce large perturbations in lipid bilayer, including membrane deformation, membrane is expansion, membrane thinning, and enhanced membrane fluctuation. Because of this permeabilization, membrane disrupted and causes an increasing of osmotic pressure inside of the cell with cell lysis [35]. Leaves of *Eucalyptus* species have been previously reported to contain various phytoconstituents that can reduce the metal salt to nanoparticles [11].

Silver nanoparticles are well documented for biomedical applications including anti-acne preparation and antibacterial efficacy due to its broad-spectrum activity against medical important pathogens, and multi-resistant strains [36]. Aim of the present study is to accomplish phytochemical analysis of *E. globulus* leaf extract using thin layer chromatography assessment. Further, to fabricate a silver nanoparticles using aqueous leaf extract of *E. globulus,* a green approach and develop antibacterial topical cream. Silver nanoparticles fortified cream characterized for physicochemical and diffusion of Ag^{+} evaluated using young pork ear skin, to predict the steady state concentration with permeability coefficient. Furthermore, the antibacterial efficacy of cream was assessed against medical important wound pathogens. Moreover, the consistency and stability was evaluated using freeze-thaw test.

2. MATERIALS AND METHODS

2.1 Materials

Silver nitrate (Mw: 169.87 g/mol), bee-wax, sodium tetraborate (Mw: 381.37 g/mol), liquid paraffin, diphenyl-1-picrylhydrazyl (DPPH), 2,2'-azino-bis(3-ethylbenzoline-6-sulfonic acid) (Mw 548.68 g/mol) (ABTS), trolox,and fibroblast L929 cells were purchased from Sigma-Aldrich (Steinheim, Singapore). Ethylene tetrazolium bromide (3-(4,5-dimethyl-2-thiazolyl)-2,5-diphenyl-2H, MTT) and trypsin were purchased from Merck (Darmstadt, Germany), Dulbecco's modified eagle medium (DMEM) and foetal bovine serum were purchased from Gibco (Paisley, UK). Bacterial including *Pseudomonas aeruginosa* ATCC 27853, *Staphylococcus aureus* ATCC 25923, and *Staphylococcus epidermidis* ATCC 12228 were obtained from culture collections laboratory, department of Pharmaceutical Science, Madhav University. All other chemicals used were of analytical grade.

2.2 Preparation and Characterization of Metallic Nanoparticles

Leaves of *E. globulus* Labill (Myrtaceae) were collected and herbarium was authenticated at Institute of Pharmacy and Research, Parul University, Gujarat, India. The leaves were rinsed with tap water and dried in oven at 40 °C for 72 h. The dried leaves were pulverized and extracted with water using maceration technique and evaluated for physicochemical, phytochemicals, antibacterial, and radical scavenging activity [37]. Moreover, the aqueous leaf extract was subjected to thin layer chromatography (mobile of phase: toluene-ethylacetate at ratio of 93:3) using silica gel G to support the results obtained from phytochemical analysis. The dried extract was used for synthesis of silver nanoparticles. In brief, 50 mg of *E. globulus* leaf aqueous extract was mixed with 179 mg of silver nitrate in a flask containing 120 mL of deionized water. The mixture was stirred and kept in dark at room temperature until the formation of dark brown color. The silver nanoparticles colloidal solution was centrifuged twice at 10000 rpm (Hermle Z 366 K, Hermle Labortechnik GmbH, Germany), 4 °C for 45 min and re-suspended in deionized water.

The surface plasmon resonance of silver nanoparticle was monitored by multi-plate UV-Vis spectrophotometer (Perkins Elmer, USA). The Ag^{+} was quantified using inductively coupled plasma optical emission spectrometry (ICP-OES), (Avio500, Perkin Elmer, USA). The morphological structure and size were studied using transmission electron microscopy (TEM), (TEM-JEOL, USA) and dynamic light scattering measurement were carried out using a Malvern DLS instrument (Zetasizer Nano ZS90, Malvern Inst. Ltd., UK). The crystallinity of lyophilized silver nanoparticles was evaluated using X-ray diffractometer (XRD - Philips- PW1710, Amsterdam). The X-ray peaks and data obtained with HighScore Plus software assigned to Debey-Scherer equation to calculate the crystallite size of silver nanoparticles.

$$D = \frac{K\lambda}{\beta \cos\theta} \quad (1)$$

Where, D is the crystallite size of silver nanoparticles, K is the Scherer constant with a

value ranging from 0.9 to 1, λ is the wavelength of the X-ray source (0.1541 nm) used in XRD, β is the full width at the half maximum of the diffraction peak and Θ is the Bragg's angle.

Structural analysis of silver nanoparticle colloidal solution was recorded using Fourier Transform Infrared Spectroscopy (FTIR, VERTEX 70, Bruker, Germany) in the range of 400–4000 cm^{-1}, with a 4 cm^{-1} resolution. The thermal behavior of lyophilized silver nanoparticle was investigated using differential scanning calorimetry (DSC 2920 calorimeter, TA Instrument, USA) and presence of any degradation during heating was confirmed using Mettler Toledo 851e TGA/SDTA (Switzerland). In brief, accurately weighed freeze dried powder samples (5 mg) was loaded in alumina crucible and heated with a rate of 10 °C/min over a temperature range of 50-800 °C, under nitrogen purge (50 ml/min), to determine loss in weight. Zeta potential was measured using Zetasizer Nano ZSP (Malvern Instruments, Worcestershire, UK) using the laser Doppler velocimetry technique [38,39].

2.3 Antibacterial Activity of Biogenic Silver Nanoparticles

Staphylococcus aureus ATCC 25923, *Staphylococcus epidermidis* ATCC 12228, and *Pseudomonas aeruginosa* ATCC 10145 were grown on tryptic soy agar at 37 °C for 24 h. All microorganisms were stored in tryptic soy agar containing 20% glycerol at –80 °C until use.

The minimum inhibitory concentration (MIC) and minimum bactericidal concentration (MBC) values of silver nanoparticles against reference strains were determined by the broth micro-dilution method according to Clinical and Laboratory Standardization Institute guidelines [40]. Briefly, serial two-fold dilutions of the silver nanoparticles were carried out in 96-well plate at concentration ranged from 0.12–66 µg/ml. An aliquot of 100 µL of diluted bacterial suspension (10^6 CFU/ml) was added in each well and incubated at 37 °C for 18 h.

2.4 Fortification of Silver Nanoparticles in Cream Base

The antibacterial cream was prepared as reported previously [36]. Briefly, 10 gm of bee's wax was mixed with hot 30 gm of liquid paraffin on water bath at 90 °C as oil phase. The aqueous phase was prepared by dissolving 0.5 gm of sodium tetraborate in required volume of double distilled water at 50 °C. An aliquot of silver nanoparticles colloidal suspension was mixed with aqueous phase and slowly added with continues stirring to the oil phase to form cream, trapped air bubbles were removed by storing the cream over night at 10 °C.

2.5 Characterization of Silver Nanoparticle Incorporated Cream

Metallic nanoparticle functionalized cream was analyzed for surface plasmon resonance using a multi-plate UV-vis spectrophotometer reader (Perkins Elmer, USA) with dilution. The viscosity of the cream was measured at room temperature using a Brookfield viscometer, (LVDV-I Prime, Brookfield, Middleboro, USA). Zeta potential and FTIR were recorded for silver nanoparticles incorporated cream as stated in previous section 2.2. The pH was determined using digital pH meter (Docu-pH+, Sartorius, Germany).

The concentration of Ag^+ in cream was quantified using ICP-OES. Briefly, appropriate volume of test samples was mixed in required volume of deionized water under mechanical shaking and extracted Ag^+ was quantified using ICP-OES.

2.6 Surface Morphology

Surface topography and elemental compositions of silver nanoparticles incorporated cream was evaluated by FESEM and EDX using JEOL-JSM5800LV (Japan). The micrographs were recorded at magnifications of 150,000X under a voltage of 3.0 kV. Moreover, the sizes of silver nanoparticles embedded in the cream were analyzed.

Surface morphology and roughness of silver nanoparticles cream was analyzed using Atomic Force Microscopy (NT-MDT Spectrum Instruments, Russia). Three-dimensional images of the film surface area (50 μm^2) were obtained in each test. Data were acquired using Easyscan-2 control software, and mean roughness (Sa) and root mean square roughness (Sq) were recorded.

2.7 Contact Angle and Surface Energy

The static contact angle of cream was evaluated by the sessile drop method, using 1 µL of probe liquid. The solvent used for the study was double distilled water, formamide, and ethylenediamine.

Three different surface regions were analyzed in triplicate.

2.8 Spreadability and Extrudability

An excess of cream (1 g) was compressed uniformly between two glass slides. The time required for the top slide to cover a specific distance under an applied force of 0.784 N was recorded and calculated using equation.

$$S = \frac{M.L}{t} \quad (2)$$

Where, M is the weight (g) tied to the upper glass slide L is the length (cm) moved on the glass slide, and t is time (s). Determinations were made in triplicates.

Cream extrudability was evaluated as previous report [1]. Briefly, silver nanoparticles incorporated cream was filled in a clean, collapsible one-ounce tube with a tip of 5 mm opening. The weight of 50 g was applied at the bottom of the tube to release cream through the opening. Extrudability was determined by weighing the amount of cream extruded through the tip. The percentage of cream extruded was calculated.

2.9 Cream Index

Optical observation method was employed to determine the instantaneous height of the emulsion and the aqueous phase inside the glass vial using scale. The cream index (CI) was calculated using the equation.

$$CI = \left(\frac{C_C}{C_T}\right) * 100 \quad (3)$$

Where, C_C is the total height of the cream layer and C_T is the total height of the emulsion layer.

2.10 Antibacterial Efficacy of Silver Nanoparticles Cream

The antibacterial efficacy of silver nanoparticles was evaluated by assessing zone of inhibition following CLSI, 2018. Briefly, petri-plates containing agar medium was seeded with a 24 h culture of the microbial strains. UV sterilized cream was placed over the inoculated agar. The inoculum size was adjusted so as to deliver final inoculums of approximately 10^6 colony-forming units (CFU)/ml, and incubated at 37 °C for 24 h. chloramphenicol (30 µg/ml) was used as positive control.

2.11 *Ex-vivo* Diffusion of Silver Nanoparticles

The *ex-vivo* diffusion study of silver nanoparticles cream was evaluated using Franz diffusion cell in triplicate. In brief, one-gram silver nanoparticles incorporated cream was accurately weighed and placed over donor compartment of Franz diffusion cell. The metallic cream was separated from diffusion media using ear skin of goat and observed for the diffusion of Ag^+. The system was maintained for 6 h at 37±0.5 °C in a thermostatically controlled water bath at 50 rpm. Aliquots of 2 mL were withdrawn at intervals of 0, 1, 2, 3, 4, 5, and 6 h, with replacement of dissolution media(phosphate buffer pH 6.8). Samples were analyzed for Ag^+ content using ICP–OES. The amount of the Ag^+ diffused was fitted to mathematical model to access the release kinetic. The cumulative quantity of Ag^+ permeating through the skin (Q) was plotted as a function of time. Skin flux was determined using Fick's law of diffusion.

$$J_{ss} = \frac{dQ_x}{A \times dt} \quad (4)$$

Where J_{ss} is the steady-state skin flux in ng/cm^2/h, dQ_x is the change in quantity of the Ag^+ passing through the skin into the receptor compartment in µg. *A* is the active diffusion area in cm^2, and *dt* is the time elapsed. The lag time (L_t, h) was calculated by extrapolating the linear region of the curve to the x-axis. The permeability coefficient (p) was calculated using equation.

$$P = \frac{J_{ss}}{S} \quad (5)$$

Where, S is the saturation solubility of the drug in the donor solution.

2.12 Cytocompatibility Silver Nano-particles Incorporated Cream

The cytocompatibility effect of cream with known silver nanoparticles concentration was investigated on fibroblast (L929) cells as previously reported [1]. In brief, cells were cultured in high glucose Dulbecco's Modified Eagle Medium (DMEM) supplemented with 10% fetal bovine serum and 100 µg/mL streptomycin and 100 µg/mL penicillin solution. Approximately 2×10^4 cells were seeded in 96–well plates (100 µL/well) and incubated at 37 °C in an incubator humidified with 5% CO_2 at 37 °C. After 24 h incubation, the culture medium was replaced with

fresh DMEM medium as negative control in triplicate. Sterile cream was dissolved in 1000 µl of DMEM under constant shaking at 150 rpm for 24 h and remaining cells were treated with elutes of silver nanoparticles from cream, and viability was analyzed using MTT assay at 570 nm.

$$Cell\ viability\ (\%) = \frac{OD_T}{OD_C} \times 100 \quad (6)$$

Where, OD_T and OD_C are absorbance of test sample and control.

2.13 Stability Study

The stability of silver nanoparticles incorporated cream was evaluated using freeze-thaw test. In brief, the metallic cream was kept in refrigerator at 4 ± 2 °C for 24 h and subsequently moved to 40 ± 2 °C for 24 h and repeated for 6 cycles and visual appearance was recorded. Furthermore, the stability of the silver nanoparticles incorporated cream was studied at 40±0.5 °C temperature and 75 % of relative humidity. The formulation was evaluated periodically for the change in color, pH, and antibacterial efficacy.

2.14 Statistical Analysis

The difference in the mean values of the data was analyzed using analysis of variance (ANOVA). Results with $p < 0.05$ were considered to be significantly different.

3. RESULTS AND DISCUSSION

Preliminary phytochemicals screening of *E. globulus* powder leaves demonstrated the presence of tannins, saponnins, carbohydrate, and glycoside. The ash values of crude leaf powder indicated the presence of inorganic composition with other impurities (Table 1). The results of physicochemical parameter assessment with reference to air dried leaf powder demonstrated 8.5, 6.5, 2.85, 0.41, and 0.35% (w/w) of loss on drying, total ash, water soluble ash, acid soluble ash, and sulphated ash, respectively. Moreover, the results of thin layer chromatography spot indicated presence of 5 compounds in aqueous fraction of *E. globulus* with R_f of 0.09, 0.16, 0.20, 0.45, and 0.94.

3.1 Radical Scavenging Efficacy of *E. globulus* Leaf Aqueous Extract

Free radicals are pre-requisite for normal cell function at physiologic concentration, however unwanted free radical can harm cellular components, such as lipid, protein, and DNA [41]. Thus, the free radical-scavenging activity of antioxidants can defend the human body from serious damage by free radicals and retards the progress of several lives threaten diseases [42]. The capability of *E. globulus* aqueous leaf extract to inhibit oxidative reaction was investigated by DPPH and ABTS

Table 1. Fluorescence characteristic of the *Eucalyptus globulus* leafpowder with different chemical reagent at 254 and 365 nm

Reagents	Visible	UV short (254 nm)	UV long (365 nm)
Powder	Dull green	Green	Brown
Conc. Nitric acid	Dull green	Dark green	Dark brown
Conc. HCl	Dull green	Dark green	Dark brown
Conc. Sulphuric acid	Dull green	Dark green	Dark brown
Ammonia	Dull green	Dark green	Dark brown
10 % Ferric chloride	Dull green	Brown	Dark brown
10 % Glacial acetic acid	Dull green	Green	Brown
Iodine solution	Dull green	Dark green	Dark brown
Picric acid	Yellowish green	Yellowish green	Brown
Dil. Sodium hydroxide	Brown	Greenish brown	Dark brown
Distilled water	Dull green	Dark green	Dark brown
Chloroform	Dull green	Dark green	Brick red
Methanol	Green	Green	Brown
Ethylacetate	Dull green	Dark green	Brick red
Acetone	Dull green	Dark green	Brick red
Benzene	Brown	Dark green	Brick red
Alcohol	Dull green	Dark green	Dark brown
Ether	Dull green	Dark green	Brick red

assay, and reduction efficacy was reported in µg/ml trolox equivalent. Aqueous leaf extract of *E. globulus* demonstrated dose dependent elevation of anti-radical activity by inhibiting DPPH and ABTS, at a maximum effect of 72.6% and 81.6 %, at a125 µg/ml. Previous report on *E. globulus* plant demonstrated that the plant is rich source of phenolic compounds that contributes for its potential antioxidant and antimicrobial efficacy [43].

3.2 Microscopy of *Eucalyptus globulus* Leaf

Transverse sectional microscopy of the *E. globulus*leaf showed dorsiventrally convex midribwith centrally located three boat shaped bicollateral meristele, and narrow isobilateral laminar extensions traversed with oil glands. Moreover, the microscopy of leaf showed upper and lower epidermis of radially elongated rectangular cells covered with very thick pale yellowish-brown cuticle and devoid of trichomes with anomocytic stomata. In addition, a differentiated mesophyll indicating palisade and spongy parenchyma was observed in leaf. Further, upper and lower palisade parenchyma contains two or three rows of thin walled, compactly arranged small palisade cells were present in the leaf. Spongy parenchyma consists of three to six layered loosely arranged parenchymatous cells were also observed within leaf. Furthermore, calcium oxalate clusters were present in both palisade and spongy parenchyma. The major portion of leaf was occupied by vascular shaped bundle towards the dorsal side. These vascular bundles are surrounded by patches of lignified pericyclic fibres.

3.3 Characterization of Metallic Nano-particles

Biogenic synthesis of silver nitrate to silver nanoparticles using *E. globulus* aqueous leaf extract fraction was visually confirmed by change of light brown to dark brown in color. The UV-vis spectra of silver nanoparticles showed characteristics surface plasmon resonance vibration at 424nm (Fig.1). The quantification of silver nanoparticles using ICP-OES revealed Ag^{+} concentration of ~71.34 ± 0.27 µg/ml. Moreover, the EDX spectral signal showed 14.7 W% of Ag^{+} in silver nanoparticles with emergence of various elements including C (48.1w%) and O (29.6w%) indicated the existence of capped compound bounded to the surface of nanoparticles (Fig.1). The results of morphological and size analysis using TEM and DLS demonstrated spherical shape of particles in range of 19 – 60 nm with effective diameter of 90 nm.

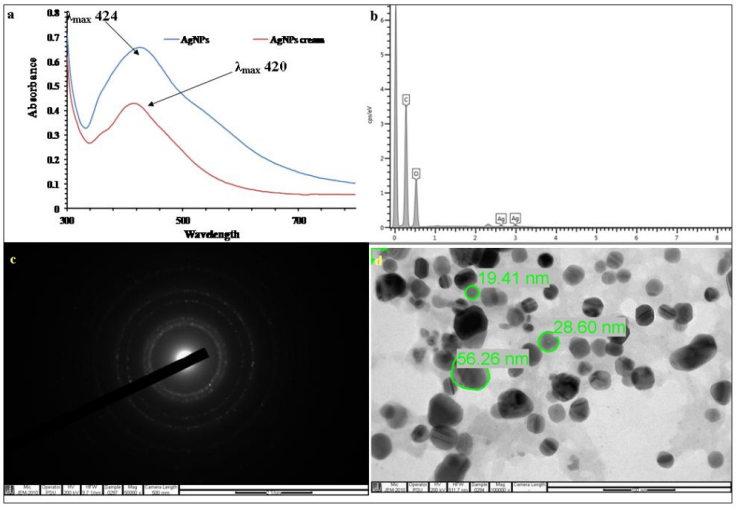

Fig.1. Surface plasmon resonance of silver nanoparticles synthesized using aqueous leaves extract of *Eucalyptus globulus* and silver nanoparticles incorporated cream using UV-vis spectrophotometer (a). Energy dispersive spectra of silver nanoparticles synthesized using aqueous leaves extract of *E. globulus* (b). Transmission electron microscopy images showing the spherical shaped silver nanoparticles at magnification of 25000 and 100000 X, indicates the presence of nanoparticles (c and d)

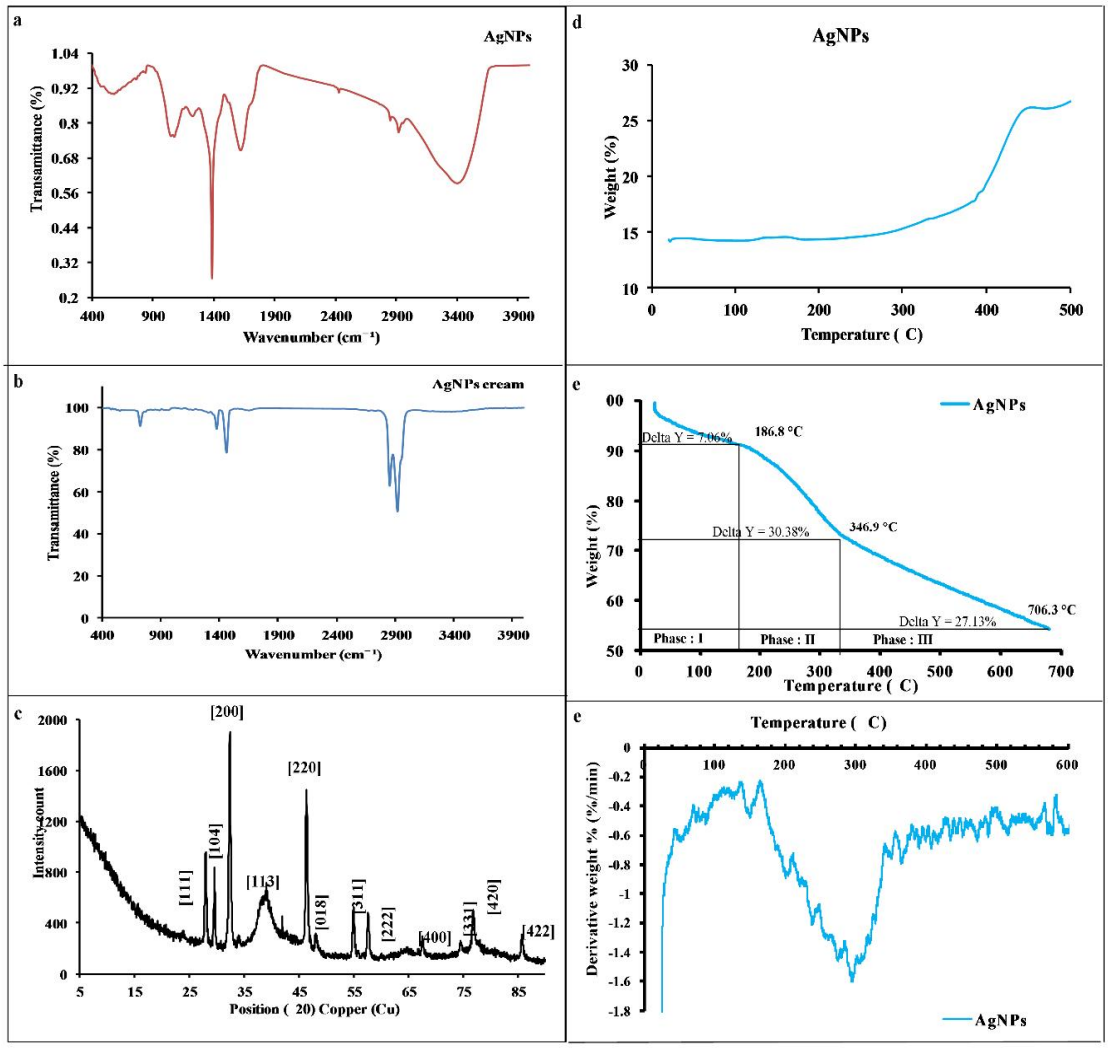

Fig. 2. Fourier transform spectra of lyophilized silver nanoparticles synthesized using aqueous leaves extract of *Eucalyptus globulus* (a), silver nanoparticles incorporated cream (b) in the range of 4000 – 400 cm^{-1}. X-ray diffraction of lyophilized silver nanoparticles synthesized using aqueous leaves extract of *E. globulus* (c). Differential scanning calorimetry spectra of lyophilized silver nanoparticles synthesized using aqueous leaves extract of *E. globulus* (d). Thermogravimetric (e) and differential thermal (f) spectra of lyophilized silver nanoparticles synthesized using aqueous leaves extract of *E. globulus*

The FTIR spectrum of silver nanoparticles is presented in Fig. 2. Distinguish vibrational bands in higher frequency range were observed for *E. globulus* aqueous leaf extract fraction as reported previously [44].The peak observed at 1312 cm^{-1} for plant extract [44] shifted to1384 cm^{-1} in silver nanoparticles was attributed to C–H bending. Silver nanoparticles demonstrated characteristic peaks at 3405–2850, 2427, 1619, 1384, 1225, 1074, 838 cm^{-1} attributed to O–H stretching, O=C=O stretching, C=C stretching, O–H bending, C–O stretching of vinyl ether, C–O stretching of primary alcohol, and C=C bending, respectively.

XRD spectra showed peak at of 27.95°(111), 32.38°(200), 46.33° (220), 54.96° (311), and 57.62° (222) corresponds to reflection planes of a face-centered cubic structure of silver, respectively [45] (Fig. 2). The average crystallite size was calculated between 20–80 nm (Table 2). The zeta potential of silver nanoparticles was

~ –33.6 mV might be due to uniform dispersion and crystallite surface repulsive force resulted from capping and stabilization of nanoparticles [46].

The thermal description of lyophilized silver nanoparticles was analyzed using DSC, TGA, and DTG and presented in Fig. 2. The exothermic and endothermic peaks at 243 and 441.67 °C, respectively observed by DSC curve corresponds to the melting point of silver [47]. Simultaneous thermogram of silver nanoparticles demonstrated putrefaction phases with a mass loss of 36.24 %. Moreover, the endothermic and exothermic peak at 316.39 and 802.61 °C correspond to – 410.22 and 101.60 J/g, respectively presented by differential thermalgravimetric analysis that revealed crystalline form of silver nanoparticles with complete degradation [48].

3.4 Antibacterial Activity of Biogenic Silver Nanoparticles

The minimum inhibitory concentration of silver nanoparticles for the tested microorganisms ranged from 0.24–30.72 µg/ml (Table 3). A previous study demonstrated that due to compositional difference in cell wall and membrane of Gram-positive and Gram-negative bacteria, silver nanoparticles shows variation in antibacterial activity. Moreover, researchers have suggested that the bonding of Ag^+ with DNA, leads to fragmentation of DNA [49]. Interaction of silver nanoparticles with cytoplasm, multiple enzymes, transporter proteins, and nucleic has also been reported as a possible mechanism leading to cell death [50].

3.5 Characterization of Silver Nanoparticle Incorporated Cream

The silver nanoparticles incorporated antibacterial cream was prepared using bees wax, liquid paraffin, and sodium tetraborate due to non-irritant and concentration dependent biocompatibility. UV-vis spectrophotometer of silver nanoparticles incorporated cream demonstrated characteristics surface plasmon resonance peak at λ_{max}420 nm (Fig.1). The results of ICP-OES indicated the concentration of 8.8µg/ml. The viscosity of cream base and silver nanoparticles was obtained as $7.89x10^5$and 8.11 $x10^5$ cPs, respectively at shear stress of 90 rpm. Silver nanoparticles embedded cream demonstrated zeta potential of – 12.83 mV might be due to aggregation in cream base. The zeta potential depends on the possible reaction between nanoparticles and the base with different charges [51].

Vibrational intensity of metallic nanomaterials incorporated cream showed similar FTIR absorption peaks to silver nanoparticles (Fig.2). The absorption peaks ranging from 724–3334 cm^{-1} was observed. The higher frequency infra-red spectrum at 3334 and 2918 cm^{-1} indicated O–H stretching due to entrapment of hydroxyl group into different mode of hydrogen bonding with cream base. Moreover, the peaks observed at 2851, 2729–2669, 1650, 1459–1375, and 724cm^{-1} ascribed to C–H stretching of alkane, doublet C–H stretching of aldehyde, C–H bending of aromatic compounds, C–H

Table 2. Particle size distribution and the inter planar spacing of silver nanoparticle

°2θ values	hkl	FWHM (*β*) in radians	Crystallite size (nm)
27.95	111	0.179	45.72
32.38	200	0.281	29.43
46.33	220	0.179	48.25
54.96	311	0.307	29.16
57.62	222	0.358	25.32

Table 3. Antibacterial activity of biogenic silver nanoparticles and silver nanoparticles incorporated cream against pathogenic microorganisms

Microorganisms	MIC/MBC (µg/mL)	Zone of inhibition (mm)
	AgNPs	AgNPs incorporated Cream
Staphylococcus aureus	2.10/33.66	19.0 ± 0.16^c
Staphylococcus epidermidis	1.05/16.8	16.0 ± 0.79^b
Pseudomonas aeruginosa	0.52/2.10	29.0 ± 0.99^b

Values are expressed as mean ± SEM (n = 6); Data was analyzed by one-way ANOVA descriptive tests$^{(ns)}$ p>0.05; **p<0.01; ***p<0.001

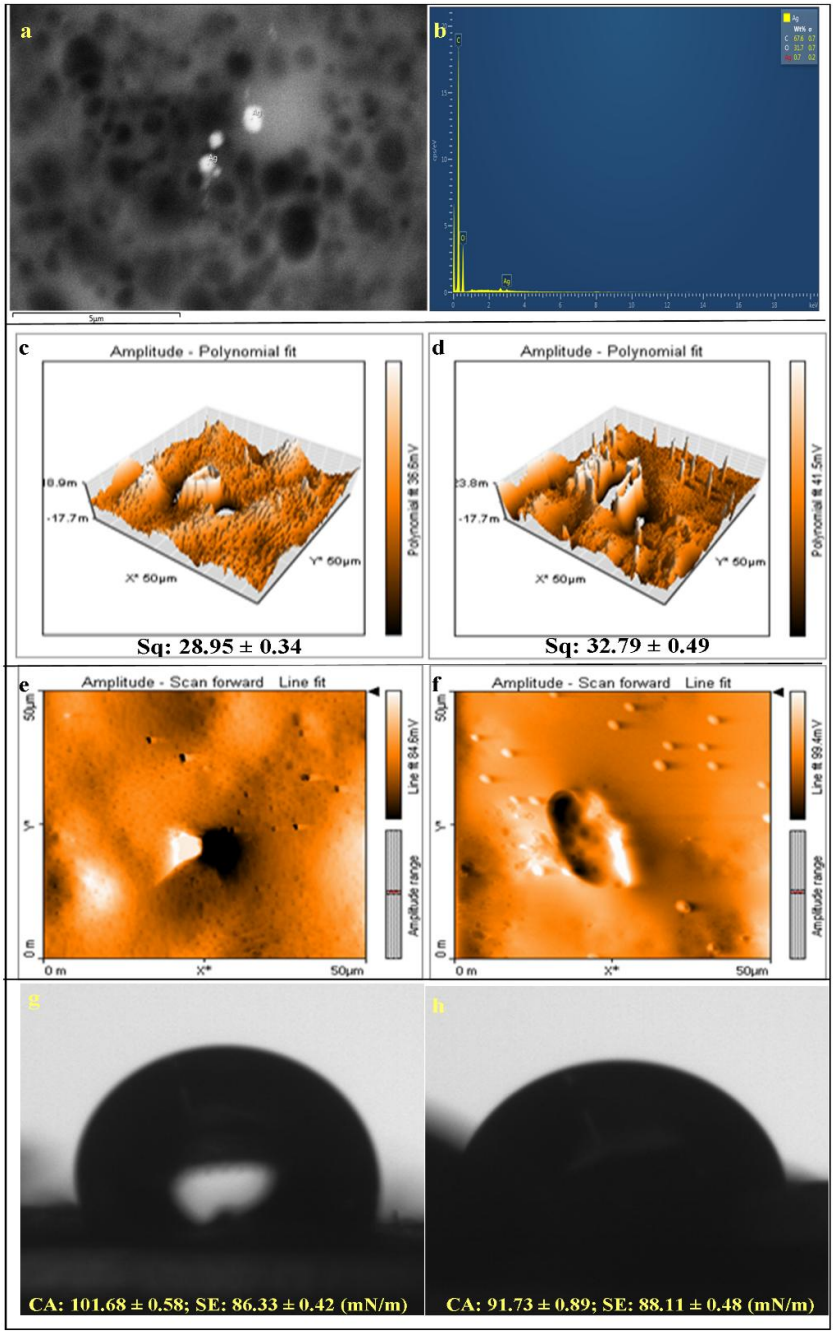

Fig. 3. Field emission scanning electron microscopy (100000 X) (a) with energy dispersive X–ray spectroscopy of silver nanoparticles (b) synthesized using aqueous leaves extract of *Eucalyptus globulus* incorporated cream. Three dimensional surface morphology and roughness of topical control cream (c), antibacterial cream functionalized with biogenic metallic nanostructured material synthesized using aqueous leaves extract of *E. globulus* (d). Two dimensional surface morphology of control cream (e) and test cream (f). Contact angle and surface energy of topical control cream (g), antibacterial cream functionalized with biogenic metallic nanostructured material synthesized using aqueous leaves extract of *E. globulus* (h)

bending of methyl group, and strong C–H bending, respectively. Similar spectral patterns were reported by researches on cream base with green synthesized silver nanoparticles [36]. FTIR analysis results demonstrated that the peaks of silver nanoparticles spectra were not affected by the addition of emulsion base cream. Furthermore, the pH of the silver nanoparticles incorporated cream was observed 6.8.

3.6 Surface Morphology

Surface topography of silver nanoparticles incorporated cream was analyzed using FESEM (Fig.3). FESEM image demonstrated spherical particles with a diameter range of 26.71–51.82 nm. The results elemental composition indicated presence of carbon (67.6 w %) and oxygen (31.7 w %) as the major constituent, compared to Ag^+ (0.7 w %). The three-dimensional Atomic force micrograph of silver nanoparticles and control cream with average roughness (Sa) and root mean square roughness (Sq) are shown in Fig. 3. The results demonstrated that the addition of silver nanoparticles did not significantly affected Sa and Sq compared to control might be due to water in oil base emulsion and proper dispersion of silver nanoparticles within base [52].

3.7 Contact Angle and Surface Energy

Wettability is an index of the hydrophilic or hydrophobic behavior and also of the ability of topical cream to adhere on skin. The contact angles of silver nanoparticles incorporated cream presented in figure3. The results demonstrated that the test and control cream are hydrophobic in nature with contact angle of ≈100° and surface energy of ~85 mN/m.

3.8 Extrudability and Spreadability

The extrudability of the silver nanoparticles incorporated cream from the tube is an important aspect for ease of its application and patient reception. The cream with high consistency may not extrude from the tube whereas, low viscous emulsion base cram may flow quickly, and hence suitable consistency is required in order to extrude the cream from the tube. The results of percentage extrudability demonstrated that the tested concentration of silver nanoparticles incorporated cream has smooth consistency (41.05±0.01), compared with cream base (43.02±0.03).

Spreadability denotes the extent of area to which the cream readily spreads on application. The silver nanoparticles incorporated cream showed spreadability with a spread time of 92.2±0.81 g/cm/s. The spreadability of the hydrophobic emulsion base cosmetics depends on the polymer concentration, polymeric chain length, viscosity, and polydispersity [1].

3.9 Cream Index

The results of creaming index were observed as 16.66 ±1.22 and 15.67±0.14 for cream base and silver nanoparticles cream, respectively. The results demonstrated that addition of silver nanoparticles in the cream base did not significantly affected the creaming index ($p < 0.05$). This might be due to chain length of emulsifying agent used in the preparation of the cream. A previous study reported that soy lecithin due to C_{16}–C_{18} chain length and cis unsaturation stabilizes better the oil in water emulsion, compared to water in oil [53].

Silver nanoparticles incorporated cream was evaluated for the antibacterial property against microorganisms commonly found in skin include *Staphylococcus aureus* ATCC 25923, *Staphylococcus epidermidis* ATCC1228, and *Pseudomonas aeruginosa* ATCC 27853. Antibacterial results revealed excellent inhibitory effects of the cream on tested microbial pathogens (Fig.4 and table 3). The results showed that silver nanoparticles embedded cream significantly ($p<0.05$) decreased the growth of tested microorganism with zone of inhibition in range of 16-29 mm.

3.10 *Ex-vivo* Diffusion of Silver Nanoparticles from Hydrophilic Matrix

Topical antibacterial efficacy of silver nanoparticles embedded cream depends on the release of Ag^+ from the emulsion base to the skin. *Ex-vivo* diffusion study results demonstrated that 2.9 ± 0.82 µg/ml of Ag^+ was released from the silver nanoparticles cream with a flux 'J' of 44.35 ng/cm^2/h and permeability coefficient of 1.29 after 4 h. These might be due to the hydrophobic nature of the polymeric matrix and concentration of silver nanoparticles present. The release mechanisms of silver nanoparticles from the cream were elucidated by fitting the release data to kinetic models including zero-order, first-order kinetic, Higuchi, Korsmeyer, and Peppas equation. The silver release follows the zero-order kinetic model with fickian diffusion (0.067)

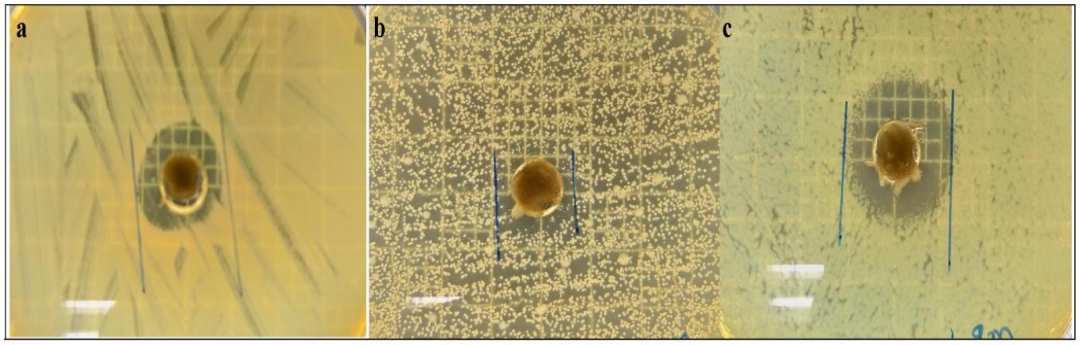

Fig. 4. Antimicrobial zone of inhibition of topical antibacterial cream functionalized with biogenic metallic nanostructured material synthesized using aqueous leaves extract of *Eucalyptus globulus* against*Staphylococcus aureus* (a), *Staphylococcus epidermidis* (b), and *Pseudomonas aeruginosa* (c)

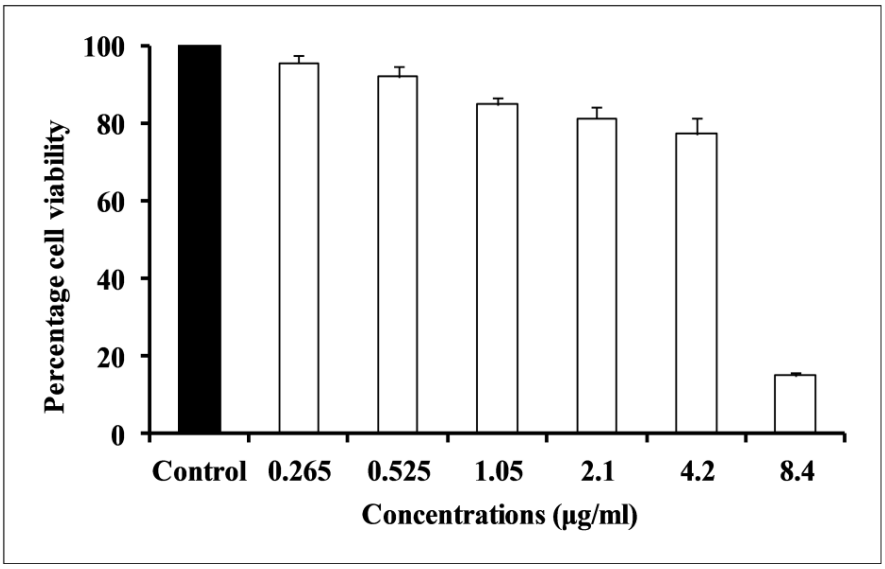

Fig. 5. Cytocompatibility on fibroblast L929 cells following exposure to elutes of silver nanoparticles incorporated topical antibacterial cream

3.11 Cell Line Biocompatibility Study

To ensure safety, efficacy, and antibacterial effect to end user the silver nanoparticles incorporated cream was tested for cytotoxicity. The effect of silver nanoparticles incorporated cream on the viability of fibroblast L929 cells was assessed with concentrations ranging from 0.265–8.4 µg/ml (Fig.5). The viability of L929 cells was not affected by tested concentrations of the cream, compared with the cell alone. The effects of the silver nanoparticles incorporated cream on the fibroblast cell at tested concentrations ranged from approximately >77.11%.These results are in agreements with previous report where eluted silver nanoparticles from surgical sutures were treated with fibroblast cells [14].

3.12 Stability Study

The freeze-thaw stability study showed no significant changes in the consistency, color, and pH. Furthermore, the antibacterial efficacy suggested that silver nanoparticles incorporated cream was stable and effective.

4. CONCLUSIONS

The study was intended to reduce and stabilize silver nitrate using aqueous extract of *E. globulus* Labill leaf and incorporate metallic nanoparticles

in a cream base for potential topical antibacterial application. The aqueous *E. globulus* leaf extract demonstrated excellent capping and stabilization of silver nanoparticles. Furthermore, the results of UV–vis, FTIR, EDX, and TEM micrograph supported the formation and stability of silver nanoparticles. In addition, the silver nanoparticles fortified cream demonstrated excellent antimicrobial activity against wound pathogen of medical importance. Moreover, this green and simple synthesis of silver nanoparticles would be suitable for the development of a biocompatible formulation for pharmaceutical and cosmetic applications.

DISCLAIMER

The products used for this research are commonly and predominantly use products in our area of research and country. There is absolutely no conflict of interest between the authors and producers of the products because we do not intend to use these products as an avenue for any litigation but for the advancement of knowledge. Also, the research was not funded by the producing company rather it was funded by personal efforts of the authors.

CONSENT

It's not applicable.

ETHICAL APPROVAL

It's not applicable.

ACKNOWLEDGEMENT

The authors would like to thanks the Department of Pharmaceutical Science, Madhav University, Sirohi, Rajasthan, India for extending laboratory facility.

COMPETING INTERESTS

Authors have declared that no competing interests exist.

REFERENCES

1. Ontong JC, Singh S, Nwabor OF, Chusri S. Voravuthikunchai SP. Potential of antimicrobial topical gel with synthesized biogenic silver nanoparticle using *Rhodomyrtus tomentosa* leaf extract and silk sericin. Biotech letters. 2020;42(12):2653-2664.
Available:https://doi.org/10.1007/s10529-020-02971-5
2. Bolla PK, Kalhapure RS, Rodriguez VA, Ramos DV, Dahl A, Renukuntla J. Preparation of solid lipid nanoparticles of furosemide-silver complex and evaluation of antibacterial activity. JDrug Deliv Sci Tech. 2019;49:6-13.
Available:https://doi.org/10.1016/j.jddst.2018.10.035
3. Ho YY, Sun DS, Chang HH. Silver nanoparticles protect skin from ultraviolet B-induced damage in mice. Int JMol Sci. 2020;21(19).
Available:https://doi.org/10.3390/ijms21197082
4. Najafi-Taher R, Ghaemi B, Kharrazi S, Rasoulikoohi S, Amani A. Promising antibacterial effects of silver nanoparticle-loaded tea tree oil nanoemulsion: a synergistic combination against resistance threat. AAPS PharmSciTech. 2018;19(3):1133-1140.
Available:https://doi.org/10.1208/s12249-017-0922-y
5. Rujido-Santos I, Naveiro-Seijo L, Herbello-Hermelo P, Barciela-Alonso MdC, Bermejo-Barrera P, Moreda-Piñeiro A. Silver nanoparticles assessment in moisturizing creams by ultrasound assisted extraction followed by sp-ICP-MS. Talanta. 2019;197:530-538.
Available:chttps://doi.org/10.1016/j.talanta.2019.01.068
6. Dhawan S, Sharma P, Nanda S. Cosmetic nanoformulations and their intended use, In: A. Nanda, S. Nanda, T.A. Nguyen, S. Rajendran, Y. Slimani (Eds.), Nanocosmetics, Elsevier. 2020;141-169.
7. Nešporová K, Pavlík V, Šafránková B, Vágnerová H, Odráška P, Žídek O, Císařová N, Skoroplyas S, Kubala L, Velebný V. Effects of wound dressings containing silver on skin and immune cells. Sci Reports. 2020;10(1):15216.
Available:https://doi.org/10.1038/s41598-020-72249-3
8. Lu PJ, Huang SC, Chen YP, Chiueh LC, Shih DYC. Analysis of titanium dioxide and zinc oxide nanoparticles in cosmetics. J Food Drug Analy. 2015;23(3):587-594.
Available:https://doi.org/10.1016/j.jfda.2015.02.009
9. Syukri DM, Nwabor OF, Singh S, Ontong JC, Wunnoo S, Paosen S, Munah S,

Voravuthikunchai SP. Antibacterial-coated silk surgical sutures by *Ex Situ* deposition of silver nanoparticles synthesized with *Eucalyptus camaldulensis* eradicates infections. JMicrobioMethods. 2020;174:105955.
Available:https://doi.org/10.1016/j.mimet.2020.105955

10. Nwabor OF, Singh S, Ontong JC, Vongkamjan K, Voravuthikunchai SP. Valorization of wastepaper through antimicrobial functionalization with biogenic silver nanoparticles, a sustainable packaging composite. WasteBiomass Valor. 2020:1-14.
Available:https://doi.org/10.1007/s12649-020-01237-5
11. Nwabor OF, Singh S, Paosen S, Vongkamjan K, Voravuthikunchai SP. Enhancement of food shelf life with polyvinyl alcohol-chitosan nanocomposite films from bioactive *Eucalyptus* leaf extracts. Food Biosci. 2020;36:100609.
Available:https://doi.org/10.1016/j.fbio.2020.100609
12. Jayeoye TJ, Eze FN, Singh S, Olatunde OO, Benjakul S, Rujiralai T. Synthesis of gold nanoparticles/polyaniline boronic acid/sodium alginate aqueous nanocomposite based on chemical oxidative polymerization for biological applications. Int JBiol Macromol. 2021;179:196-205.
Available:https://doi.org/10.1016/j.ijbiomac.2021.02.199
13. Kokura S, Handa O, Takagi T, Ishikawa T, Naito Y, Yoshikawa T. Silver nanoparticles as a safe preservative for use in cosmetics. Nanomed Nanotech Biol Med. 2010;6(4):570-574.
Available:https://doi.org/10.1016/j.nano.2009.12.002
14. Syukri DM, Nwabor OF, Singh S, Voravuthikunchai SP. Antibacterial functionalization of nylon monofilament surgical sutures through *in situ* deposition of biogenic silver nanoparticles. SurfaceCoat Tech. 2021;127090.
Available:https://doi.org/10.1016/j.surfcoat.2021.127090
15. Eze FN, Nwabor OF. Valorization of Pichia spent medium via one-pot synthesis of biocompatible silver nanoparticles with potent antioxidant, antimicrobial, tyrosinase inhibitory and reusable catalytic activities, Mat Sci Eng: C. (2020);115:111104.
Available:https://doi.org/10.1016/j.msec.2020.111104.
16. John MS, Nagoth NJ, Ramasamy KP, Patirzia B, Matteo M, Alessio M, Andrea T, Pietro L, Gabriele G, Antonino N, Cristina M, Sandra P Horizontal gene transfer and silver nanoparticles production in a new Marinomonas strain isolated from the Antarctic psychrophilic ciliate Euplotes focardii, Scient Report. 2020;10:10218.
Available:https://doi.org/10.1038/s41598-020-66878-x
17. Dey B, Mitra A. Chemo-profiling of *Eucalyptus* and study of its hypoglycemic potential. World J Diabetes. 2013;4(5):170-176.
Available:https://dx.doi.org/10.4239%2Fwjd.v4.i5.170
18. Bhuyan DJ, Sakoff J, Bond DR, Predebon M, Vuong QV, Chalmers AC, van Altena IA, Bowyer MC, Scarlett CJ. *In vitro* anticancer properties of selected *Eucalyptus* species, *In vitro* cellular and developmental biology. Animal. 2017;53(7):604-615.
19. Mahmoudzadeh-Sagheb H, Heidari Z, Bokaeian M, Moudi B. Antidiabetic effects of *Eucalyptus globulus* on pancreatic islets: a stereological study. Folia Morphologica. 2010;69(2):112-8.
20. Bachir RG, Benali M. Antibacterial activity of the essential oils from the leaves of *Eucalyptus globulus* against *Escherichia coli* and *Staphylococcus aureus*. Asian Pacific JTrop Biomed. 2012;2(9):739-742.
Available:https://dx.doi.org/10.1016%2FS2221-1691(12)60220-2
21. Salari MH, Amine G, Shirazi MH, Hafezi R, Mohammadypour M. Antibacterial effects of *Eucalyptus globulus* leaf extract on pathogenic bacteria isolated from specimens of patients with respiratory tract disorders. Clinical Microbiol Infec. 2006;12(2):194-196.
Available:https://doi.org/10.1111/j.1469-0691.2005.01284.x
22. Hukkeri VI, Karadi R, Akki KS, Savadi RV, Jaiprakash B, Kuppast IJ, Patil MB. Wound healing property of *Eucalyptus globulus* L. leaf extract'. 2002;39:481-483.
23. Saporito F, Sandri G, Bonferoni MC, Rossi S, Boselli C, Icaro Cornaglia A, Mannucci B, Grisoli P, Vigani B, Ferrari F, Essential oil-loaded lipid nanoparticles for wound healing. Int J Nanomed.2017;13:175-186.

Available:https://doi.org/10.2147/ijn.s152529

24. Kubera Sampath Kumar S, Prakash C, Ramesh P, Sukumar N, Balaji J, Palaniswamy NK. Study of wound dressing material coated with natural extracts of *Calotropis Gigantean*, *Eucalyptus globulus* and buds of *Syzygium Aromaticum* solution enhanced with rhEGF (REGEN-D™ 60). J Natural fibers. 2020;1-14.
Available:https://doi.org/10.1080/15440478.2020.1726239
25. Navayan A, Moghimipour E, Khodayar M, Vazirianzadeh B, Siahpoosh A, Valizadeh M, Mansourzadeh Z. Evaluation of the mosquito repellent activity of nano-sized microemulsion of *Eucalyptus globulus* essential oil against culicinae. Jundishapur JNatural Pharm Products. 2017;12(4):e55626.
Available:https://dx.doi.org/10.5812/jjnpp.55626
26. Ibáñez M, Blázquez M. Post-emergence herbicidal activity of *Eucalyptus globulus* Labill. Essential oil. 2018.
Available:http://dx.doi.org/10.3390/mol2net-04-05374
27. Puig CG, Reigosa MJ, Valentão P, Andrade PB, Pedrol N. Unravelling the bioherbicide potential of *Eucalyptus globulus* Labill: biochemistry and effects of its aqueous extract. PLoS One. 2018;13(2):e0192872.
Available:https://doi.org/10.1371/journal.pone.0192872
28. Adenubi OT, Abolaji AO, Salihu T, Akande FA, Lawal H. Chemical composition and acaricidal activity of *Eucalyptus globulus* essential oil against the vector of tropical bovine piroplasmosis, *Rhipicephalus* (Boophilus) annulatus. Experiment Applied Acarology. 2021;83(2):301-312.
Available:https://doi.org/10.1007/s10493-020-00578-z
29. Böhm L, Arismendi N, Ciampi L. Nematicidal activity of leaves of common shrub and tree species from southern chile against meloidogyne hapla. Cienciae Investigación Agraria. 2009;36(2):249-258.
Available:http://dx.doi.org/10.4067/S0718-16202009000200009
30. Vecchio M, Loganes C, Minto C. Beneficial and healthy properties of *Eucalyptus* plants: a great potential use. Open Agriculture J. 2016;10:52-57.
Available:http://dx.doi.org/10.2174/1874331501610010052
31. Dhakad AK, Pandey VV, Beg S, Rawat JM, Singh A. Biological, medicinal and toxicological significance of *Eucalyptus* leaf essential oil: a review. Journal of science food agriculture. 2018;98(3):833-848.
Available:https://doi.org/10.1002/jsfa.8600
32. Mishra AK, Sahu N, Mishra A, Ghosh AK, Jha S, Chattopadhyay P. Phytochemical screening and antioxidant activity of essential oil of *Eucalyptus* leaf. Pharmacog J. 2010;2(16):25-28.https://doi.org/10.1016/S0975-3575(10)80045-8
33. Kaur S, Gupta S, Gautam P. Phytochemical analysis of *Eucalyptus* leaves extract. J Pharmacog Phytochem. 2019;8:2442-2446.
34. Ghisalberti EL. Bioactive acylphloroglucinol derivatives from *Eucalyptus* species. Phytochem. 1996;41(1):7-22.
Available:https://doi.org/10.1016/0031-9422(95)00484-x
35. Tan HB, Liu HX, Zhao LY, Yuan Y, Li BL, Jiang YM, Gong L, Qiu XS. Structure-activity relationships and optimization of acyclic acylphloroglucinol analogues as novel antimicrobial agents. Europ J Med Chem. 2017;125:492-499.
Available:https://doi.org/10.1016/j.ejmech.2016.09.054
36. Odeniyi MA, Okumah VC, Adebayo-Tayo BC, Odeniyi OA. Green synthesis and cream formulations of silver nanoparticles of *Nauclea latifolia* (African peach) fruit extracts and evaluation of antimicrobial and antioxidant activities. Sustainable Chem Pharm. 2020;15:100197.
Available:https://doi.org/10.1016/j.scp.2019.100197
37. Nwabor OF, Singh S, Marlina D, Voravuthikunchai SP. Chemical characterization, release, and bioactivity of *Eucalyptus camaldulensis* polyphenols from freeze-dried sodium alginate and sodium carboxymethyl cellulose matrix. Food Qual Safety. 2020;4(4):203-212.
Available:https://doi.org/10.1093/fqsafe/fyaa016
38. Singh S, Nwabor OF, Ontong JC, Voravuthikunchai SP. Characterization and assessment of compression and compactibility of novel spray-dried, co-processed bio-based polymer. J Drug Del Sci Tech.2020; 56: 101526.

Available:https://doi.org/10.1016/j.jddst.2020.101526.

39. Singh S, Nwabor OF, Ontong JC, Kaewnopparat N, Voravuthikunchai SP. Characterization of a novel, co-processed bio-based polymer, and its effect on mucoadhesive strength. Int J Biol Macromol. 2020;145:865-875. Available:https://doi.org/10.1016/j.ijbiomac.2019.11.198
40. Performance standards for antimicrobial susceptibility testing. In clinical and laboratory Standards Institute, approved standard, 27th edn. informational supplement,Wayne, Pennsylvania 19087, USA. 2018;M100-S28.
41. Naveen K, Roshan DP, Manjul PS, Anita Singh, Naheed WS, Gulzar A, Sudarshan KS. Phyto-physicochemical investigation of leaves of *Plectranthus amboinicus* (Lour) Spreng. Pharmacog J. 2010a;2(13):536. Available:https://doi.org/10.1016/S0975-3575(10)80057-4
42. Naveen K, Roshan DP, Manjul PS, Anita Singh, Naheed WS, Gulzar A, Sudarshan KS. Antioxidant potential of leaves of *Plectranthus amboinicus* (Lour) Spreng. Der Pharmacia Lettre. 2010b;2(4):240-245.
43. Dezsi Ș, Bădărău AS, Bischin C, Vodnar DC, Silaghi-Dumitrescu R, Gheldiu AM, Mocan A, Vlase L. Antimicrobial and antioxidant activities and phenolic profile of *Eucalyptus globulus* Labill. and *Corymbia ficifolia* (F. Muell.) KD Hill & LAS Johnson leaves. Molecules. 2015;20(3):4720-4734. Available:https://doi.org/10.3390/molecules20034720
44. Gullón B, Gullón P, Lú-Chau TA, Moreira MT, Lema JM, Eibes G. Optimization of solvent extraction of antioxidants from *eucalyptus globulus* leaves by response surface methodology: characterization and assessment of their bioactive properties. Industrial Crops Prod. 2017;108:649-659. Available:https://doi.org/10.1016/j.indcrop.2017.07.014
45. Yahyaei B, Manafi S, Fahimi B, Arabzadeh S, Pourali P. Production of electrospun polyvinyl alcohol/microbial synthesized silver nanoparticles scaffold for the treatment of fungating wounds. Applied Nanosci. 2018;8(3):417-426.https://doi.org/10.1007/s13204-018-0711-2
46. Parameshwaran R, Kalaiselvam S, Jayavel R. Green synthesis of silver nanoparticles using *beta vulgaris*: role of process conditions on size distribution and surface structure. Materials Chem Phy. 2013;140(1):135-147. Available:https://doi.org/10.1016/j.matchemphys.2013.03.012
47. Kota S, Dumpala P, Anantha RK, Verma MK, Kandepu S. Evaluation of therapeutic potential of the silver/silver chloride nanoparticles synthesized with the aqueous leaf extract of *Rumex acetosa*. Scientific Rep. 2017;7(1):11566. Available:https://doi.org/10.1038/s41598-017-11853-2
48. Majeed Khan MA, Kumar S, Ahamed M, Alrokayan SA, Alsalhi MS. Structural and thermal studies of silver nanoparticles and electrical transport study of their thin films. Nanoscale Res letters. 2011;6(1):434-434. Available:https://dx.doi.org/10.1186%2F1556-276X-6-434
49. Khan BF, Hamidullah, Dwivedi S, Konwar R, Zubair S, Owais M. Potential of bacterial culture media in biofabrication of metal nanoparticles and the therapeutic potential of the as-synthesized nanoparticles in conjunction with artemisinin Against MDA-MB-231 breast cancer cells. J Cell Physiol. 2019; 234(5): 6951-6964. Available:https://doi.org/10.1002/jcp.27438
50. Gomaa EZ. Silver nanoparticles as an antimicrobial agent: A case study on *Staphylococcus aureus* and *Escherichia coli* as models for Gram-positive and Gram-negative bacteria. The J General ApplMicrob. 2017; 63(1):36-43. Available:https://doi.org/10.2323/jgam.2016.07.004
51. Wang T, Zhang F, Zhao R, Wang C, Hu K, Sun Y, Politis C, Shavandi A, Nie L. Polyvinyl alcohol/sodium alginate hydrogels incorporated with silver nanoclusters via green tea extract for antibacterial applications. Desigend Monomers Polym. 2020;23(1):118-133. Available:https://doi.org/10.1080/15685551.2020.1804183
52. Anirudhan TS, Deepa JR, Christa J. Nanocellulose/Nanobentonite composite anchored with multi-carboxyl functional groups as an adsorbent for the effective removal of cobalt(II) from nuclear industry wastewater samples. J Colloid Interface Sci. 2016;467:307-320. Available:https://doi.org/10.1016/j.jcis.2016.01.023

53. Djiobie Tchienou GE, Tsatsop Tsague RK, Mbam Pega TF, Bama V, Bamseck A, Dongmo Sokeng S, Ngassoum MB. Multi-response optimization in the formulation of a topical cream from natural ingredients. Cosmetics. 2018;5(1):7. Available:https://doi.org/10.3390/cosmetics5010007

Peer-review history:
The peer review history for this paper can be accessed here:
http://www.sdiarticle4.com/review-history/69139